Statistical and Block Copolymers of 7-Oxabicyclo[2.2.1]heptane with Tetrahydrofuran. Conditions of Copolymerization and Distribution of the Promesogenic Units

Julia Pretula, Krzysztof Kaluzynski, Ryszard Szymanski, and Stanislaw Penczek*

Centre of Molecular and Macromolecular Studies, Polish Academy of Sciences, 90-363 Lodz, Sienkiewicza 112, Poland

Received August 14, 1995; Revised Manuscript Received April 25, 1996[⊗]

ABSTRACT: Statistical and block copolymerizations of tetrahydrofuran (**T**) and 7-oxabicyclo[2.2.1]heptane (**B**) (providing promesogenic units) have been studied. The structure of the active species and their concentration and stability were determined by the ion-trapping method, and on this basis the reactivities of **T** and **B** active species were estimated. **B** active species are about 10 times more reactive than **T** ones, reflecting the higher ring strain of **B**, due to the presence of "two rings in one". This high reactivity of **B** active species leads to the enhanced chain transfer to the poly-**T** units and, therefore, eliminates the possibility of preparing pure di- or triblock copolymer (by copolymerization). The estimated ratio of the rate constants of reaction between **B** active species and **B** monomer or **T** repeating unit (in homosequences) is equal to 3 at typical copolymerization conditions. When, however, polymerization of **B** was started from the active poly-**T** precursor, then multiblock copolymers were prepared. For instance, a multiblock copolymer of the average structure $[(\mathbf{B})_{9.2}(\mathbf{T})_{17.2}]_n$ was prepared in CH_3NO_2 solution, from which copolymer precipitates.

Introduction

Polymers of oxygen-bridged bicyclic ethers such as 7-oxabicyclo[2.2.1]heptane (**B**) and several of its substituted derivatives were prepared and a number of these polymers were characterized in the past. Thus, the parent polymer was described in the open literature for the first time by Wittbecker, Hall, and Campbell as a high-melting, crystalline product, with the 1,4-*trans* configuration for the cyclohexane ring.[1] Polymers of the corresponding *endo*- and *exo*-2-methyl derivatives (**BN** and **BX**, respectively) were first shown to have exclusively the 1,4-*trans* configuration for the cyclohexane ring,[2] although in more recent studies, when the more powerful NMR technique (500 MHz) was used,[3] some irregular repeating units were identified in the poly-**BX**.

Kops showed that polymers of **BX** and **BN** exhibit liquid crystallinity,[3] whereas Percec analyzed the general conditions required for promesogenic flexible molecules to provide LC properties, pointing out that polymers of bicyclic ethers were known for a long time before their LC properties became recognized.[4]

Copolymerization of **B** with ethylene oxide has been the only copolymerization of **B** studied in more detail.[5] Conditions of preparation of the fiber-forming terpolymers **B**−ethylene oxide−THF and **B**−THF copolymers have been described more recently.[6] We published a work in which an attempt was made to prepare periodic $[-(THF)_1-\mathbf{B}_n-]_m$ copolymers.[7]

In the present paper, the second one of a series devoted to copolymers of **B** and its *endo*- and *exo*-2-methyl derivatives (**BN** and **BX**), we describe conditions and results of synthesis of the statistical and block copolymers of **B** and **T**. We use the term "statistical" and not "random" because the copolymers obtained were not exactly random and exhibited some tendency to alternation.[7] On the basis of the available data, we estimated also the basic kinetic parameters, including a few rate constants, not known before. The LC properties of these and other related copolymers, and particularly the proportion of the LC structures as a function of the size of the mesogenic blocks and their distribution, will be published separately.

Experimental Section

The comonomers—**B** (Aldrich) and **T** (POCh, Poland)—were purified by distillation from CaH_2 and were finally dried and kept over Na/K alloy. Dichloromethane and nitromethane, after purifying in a standard way, were dried with CaH_2. Dichloromethane was finally dried over Na mirror. Initiators: trifluoromethanesulfonic anhydride (Aldrich) was used after being freshly distilled on the vacuum line, and benzoylium hexafluoroantimonate was prepared and used as described previously.[8] Silver hexafluoroantimonate (Aldrich) was used without purification.

Polymerizations were carried out in sealed vacuum ampules with breakseals. Solvent and reagents were mixed at low temperature and then the temperature was rapidly raised to the desired level. Polymerizations were killed after the desired reaction time with freshly distilled tributylphosphine (Aldrich) or with NH_3/CH_3OH solution.

Poly-**T** terminated on both ends with iodide groups was prepared by reaction of living poly-**T** (initiated with trifluoromethanesulfonic anhydride) and tetra-*n*-octylammonium iodide.

The composition and microstructure of the copolymers were determined from ^1H and ^{13}C NMR spectra registered in benzene/phenol (4:1 w/w) solution on Bruker AC-200 or Bruker MSL-300 spectrometers, operating at 200 or 300 MHz, respectively (^1H spectra). ^{13}C NMR spectra were recorded with inverted gated decoupling, allowing a quantitative analysis of fractions of different diads and triads. Chemical shifts were computed assuming benzene signal position at $\delta = 128.7$ ppm. The reported fractions of different sequences were computed from the least squares fit of predicted intensities of different signals to the observed ones.

End groups were determined from ^1H NMR and/or UV−vis spectra. The OH groups were determined from ^1H NMR spectra in chloroform containing an excess of trifluoroacetic anhydride, converting OH groups to the ester groups, according to the method described previously.[9]

An ion-trapping method was used to determine active chain end groups of some polymers and copolymers after reaction with tributylphosphine.[10] Tributylphosphine was used be-

[⊗] Abstract published in *Advance ACS Abstracts,* June 15, 1996.

S0024-9297(95)01183-1 CCC: $12.00

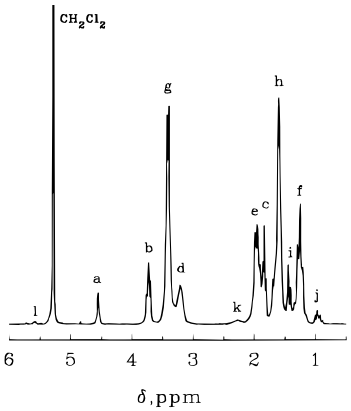

Figure 1. ^{1}H NMR spectrum of the copolymerization mixture of **T** and **B** in CH_2Cl_2 solution initiated with $PhCOSbF_6$ and terminated with $(nC_4H_9)_3P$. Copolymerization conditions: 25 °C, $[I]_0 = 0.04$ mol L^{-1}, $[\mathbf{T}]_0 = 4.70$ mol L^{-1}, $[\mathbf{B}]_0 = 3.09$ mol L^{-1}. Assignment of signals: (a) $-OCH-$ in **B**; (b) $-OCH_2-$ in **T**; (c): $-CH_2CH_2CH_2CH_2-$ in **T**; (d): $-CH(-CH_2CH_2-)_2-CH-$ in **B** copolymer units; (e) axial protons of **B** units: $[-OCH(-CH_2CH_2-)_2CH-]$; (f) equatorial protons of the same units; (g) $-OCH_2CH_2CH_2CH_2O-$ in **T** units; (h) $-OCH_2CH_2CH_2-CH_2O-$ in **T** units; (i) $\sim P^+(CH_2CH_2CH_2CH_3)_3$; (j) $\sim P^+(CH_2CH_2-CH_2CH_3)_3$; (k): $\sim P^+(CH_2CH_2CH_2CH_3)_3$ end groups; (l) olefinic protons of cyclohexene end groups.

cause it allows the determination of the concentrations of protons in solution, in contrast to easier to handle triphenylphosphine.

Molecular weights of copolymers soluble in **T** were determined from GPC measurements applying calibration for polystyrene. In addition, vapor pressure osmometry measurements of some samples were performed in CH_2Cl_2 solution on a Knauer osmometer at 25 °C.

Results and Discussion

Copolymerization Conditions and Livingness. Homopolymerization of **T**, when conducted in the presence of a stable counterion (e.g., AsF_6^- or SbF_6^-), is known to proceed as a living process.[11] However, reversibility of polymerization broadens the molecular weight distribution. The extent of broadening depends on the importance of the reversibility, influenced by $[\mathbf{T}]_0$, temperature, and the solvent properties.

Polymerization of **B**, described in ref 1, was not studied in detail, due to the insolubility of poly-**B**. It was known that the highest molecular weights were observed with PF_5 as initiator in nitrobenzene solution, although only $FeCl_3/SOCl_2$, $SbCl_5$, BF_3/methyloxirane, and $SnCl_4/CH_3COCl$ were tested as other initiators.[1] The available data on the copolymerization with **T** from refs 1 and 6 are rather scarce, and only the T_m and some other physical properties of copolymers characterized by their total composition are given.

Copolymers of **B** and **T** were prepared at conditions corresponding to the living polymerization of **T** and polymerizations were conducted to higher yields than in our previous paper, where reactivity ratios were estimated.[7] Depending on the copolymerization conditions, the final products are either soluble or insoluble in the polymerization mixture.

We studied copolymerization, as indicated in the Introduction, in order to prepare copolymers with different total proportions of comonomers and with different distributions of mesogenic units, provided by **B**. Therefore, the products we prepared vary from statistical with some tendency to alternating structures ($r_1r_2 < 1$)[7] to block copolymers containing longer homosequences.

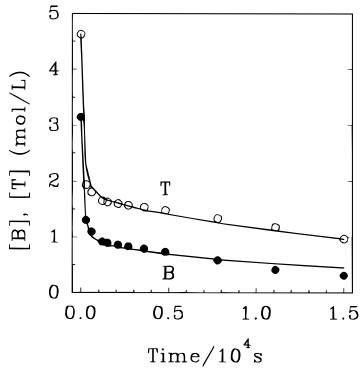

Figure 2. Kinetics curves of conversion of **T** and **B** during statistical copolymerization at 25 °C in CH_2Cl_2 (initiator $PhCOSbF_6$, $[I]_0 = 0.086$ mol L^{-1}, $[\mathbf{T}]_0 = 4.63$ mol L^{-1}, $[\mathbf{B}]_0 = 3.15$ mol L^{-1}).

In Figure 1, the ^{1}H NMR spectrum of the copolymerization mixture and the respective assignments for monomers and polymers are given. In Figure 2, typical kinetics curves of conversion of both **B** and **T** during statistical copolymerization are shown (on the basis of monomer as well as polymer unit concentrations, monitored directly by ^{1}H NMR during copolymerization). As follows from Figure 2, both monomers copolymerize with comparable rates.

Kinetics of Statistical Copolymerization. The preliminary kinetic analysis of the statistical copolymerization carried out at 30 °C in CH_2Cl_2 solution allowed us to estimate some values of the rate constants (or their ratios) of reactions operating in the copolymerization system. This estimation was performed by fitting the calculated concentrations of the comonomers to the experimental data. The assumed scheme of copolymerization was as follows:

$$I + \mathbf{B} \xrightarrow{\text{fast}} \sim\mathbf{B}^* \quad (1)$$

$$I + \mathbf{T} \xrightarrow{\text{slow}} \sim\mathbf{T}^* \quad (2)$$

$$\sim\mathbf{B}^* + \mathbf{B} \underset{k_{-BB}}{\overset{k_{BB}}{\rightleftharpoons}} \sim\mathbf{BB}^* \quad (3)$$

$$\sim\mathbf{B}^* + \mathbf{T} \underset{k_{-BT}}{\overset{k_{BT}}{\rightleftharpoons}} \sim\mathbf{BT}^* \quad (4)$$

$$\sim\mathbf{T}^* + \mathbf{B} \underset{k_{-TB}}{\overset{k_{TB}}{\rightleftharpoons}} \sim\mathbf{TB}^* \quad (5)$$

$$\sim\mathbf{T}^* + \mathbf{T} \underset{k_{-TT}}{\overset{k_{TT}}{\rightleftharpoons}} \sim\mathbf{TT}^* \quad (6)$$

$$\sim\mathbf{B}^* \xrightarrow{k_{ter}} \sim\mathbf{B} + \text{“}H^+\text{”} \quad (7)$$

$$\text{“}H^+\text{”} + \mathbf{B} \xrightarrow{k_{rei}} \sim\mathbf{B}^* \quad (8)$$

$$(\text{“}H^+\text{”} + \mathbf{T} \not\rightarrow \sim\mathbf{T}^*) \quad (9)$$

Termination does not take place in **T** polymerization carried out with stable anions, as already established in the early works describing polymerization of THF as a living process.[12−14] Therefore it was assumed that only **B**-type active species undergo termination by deprotonation with formation of the CC (cyclohexenyl) double bond, which was observed at $\delta = 5.6$ ppm in the

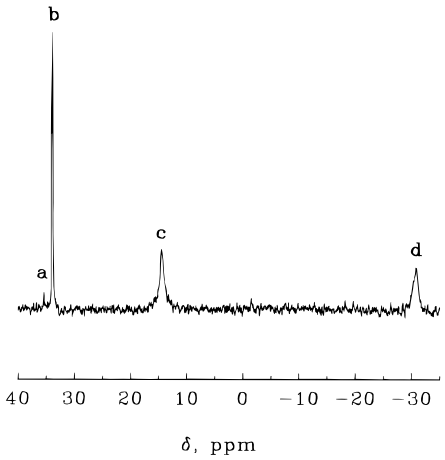

Figure 3. ^{31}P NMR spectrum of the statistical copolymerization mixture of **B** and **T** killed with $(nC_4H_9)_3P$ after 660 s. Copolymerization conditions: solvent CH_2Cl_2, −25 °C, initiator $PhCOSbF_6$, $[I]_0 = 0.067$ mol L^{-1}, $[\mathbf{T}]_0 = 2.08$ mol L^{-1}, $[\mathbf{B}]_0 = 1.46$ mol L^{-1}. (a) $-OCH(CH_2CH_2)_2CHP^+nC_4H_9)_3$; (b) $-OCH_2CH_2CH_2CH_2P^+nC_4H_9)_3$; (c) $HP^+nC_4H_9)_3$; (d) $P(nC_4H_9)_3$.

^{1}H NMR spectrum. As initiation of **T** with protonic acids is rather ineffective, we assumed that only **B** can react with protons reinitiating copolymerization.

Thus, we formulated the corresponding differential equations for changes of concentrations of comonomers and different types of active species, according to eqs 1−9. Assuming steady-state conditions for the concentrations of different active species and assuming that the conditional probabilities of preceding units of a given kind in the copolymer by units of the same kind are independent of the chain position, it was possible to solve numerically the set of differential equations describing copolymerization. Details are given in the Appendix. Consequently, by fitting the experimentally determined concentrations of comonomers at different reaction times to the conversion curves obtained by the numerical integration of the formulated set of differential equations, we could estimate some rate constants of the assumed reaction scheme, some reactivity ratios, and other ratios of rate constants. These estimates are as follows (30 °C, CH_2Cl_2 solution): $k_{TT} = 2.2 \times 10^{-2}$ (±20%) mol^{-1} L s^{-1} (this value is slightly lower than the reported rate constant of homopolymerization of **T**: $k_p = 3.9 \times 10^{-2}$ mol^{-1} L s^{-1} at 25 °C),[15] $k_{BB}/k_{TT} = 10$ (±30%), $r_T = k_{TT}/k_{TB} = 0.65$ (±30%), $r_B = k_{BB}/k_{BT} = 0.99$ (±20%), $k_{ter} = 2 \times 10^{-2}$ (±30%) s^{-1}, $k_{rei} < 10^{-5}$ mol^{-1} L s^{-1}.

The above estimates confirm our observations that the bicyclic active center ∼**B*** is much more reactive than the **T**-type one. Because of this high reactivity, the termination reaction cannot be neglected. Reinitiation is rather ineffective and it can explain low conversions in some experiments.

Active Species and Their Stabilities. Application of the $(nC_4H_9)_3P$-ion-trapping method[9] allowed the determination of the concentrations of both active species, derived from **B** and **T**, respectively, as well as the presence of protons formed in termination and bound to some nucleophilic centers in the system. The $^{31}P\{^1H\}$ NMR spectrum of the copolymerization of **B** with **T** killed with $(nC_4H_9)_3P$ is given in Figure 3. There is one signal corresponding to the unreacted (taken in excess) tributylphosphine and signals corresponding to the products of reaction of phosphine with active species derived from **B** or **T**. The following chemical shifts have been observed: tributylphosphine, $\delta = -30.9$ ppm; **T**-type active species converted to the tetraalkylphosphonium cation, $\delta = 33.8$ ppm; **B**-type active species converted to the tetraalkylphosphonium cation, $\delta = 35.3$ ppm; protonated phosphine, $\delta = 14.4$ ppm.

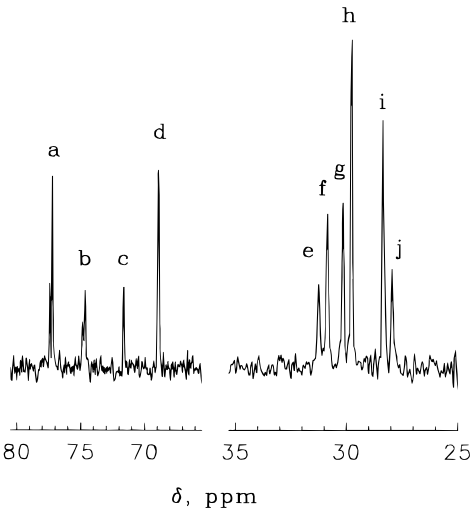

Figure 4. ^{13}C NMR spectrum of 1:1 statistical copolymer of **T** with **B**. Copolymerization conditions: temperature 0 °C, solvent CH_2Cl_2, initiator $PhCOSbF_6$, $[I]_0 = 0.039$ mol L^{-1}, $[\mathbf{T}]_0 = 2.33$ mol L^{-1}, $[\mathbf{B}]_0 = 2.52$ mol L^{-1}, reaction time 145 h. Assignment of signals: $-\mathbf{T}-O-C^{(a)}H(C^{(h)}H_2C^{(h)}H_2)_2C^{(a)}H-O-\mathbf{T}-$; $-\mathbf{T}-O-C^{(a)}H(C^{(g)}H_2C^{(f)}H_2)_2C^{(b)}H-O-\mathbf{B}-$; $-\mathbf{B}-O-C^{(b)}H(C^{(e)}H_2C^{(e)}H_2)_2C^{(b)}H-O-\mathbf{B}-$; $-\mathbf{B}-O-C^{(d)}H_2C^{(i)}H_2C^{(i)}H_2C^{(d)}H_2-O-\mathbf{B}-$; $-\mathbf{B}-O-C^{(d)}H_2C^{(i)}H_2C^{(j)}H_2C^{(c)}H_2-O-\mathbf{T}-$; $-\mathbf{T}-O-C^{(c)}H_2C^{(j)}H_2C^{(j)}H_2C^{(c)}H_2-O-\mathbf{T}-$.

Knowing the concentration of the added phosphine and comparing the integrals of different signals, the concentrations of different types of active species at different stages of copolymerization were estimated. During copolymerization, the ratio of the active species from **B** and **T** (∼**B*** and ∼**T***, respectively) does not change substantially. Thus, for copolymerization at 25 °C and starting monomer concentrations $[\mathbf{B}]_0 = 3.09$ and $[\mathbf{T}]_0 = 4.70$ mol L^{-1}, initiated with $[(C_6H_5COSbF_6]_0 = 3.8 \times 10^{-2}$ mol L^{-1} in CH_2Cl_2 solvent, integration of the ^{1}H NMR spectra gives the concentration of the $(nC_4H_9)_3P$ added, and the ^{31}P NMR spectrum, taking $(nC_4H_9)_3P$ as an internal standard, gives the concentrations of both active species. At 53% comonomer conversion, the sum of these concentrations gives ∼35% of the initial concentration of initiator; the rest is found as the protonated phosphine, $H-P^+(nC_4H_9)_3$. This proportion of the protonated phosphine increases with conversion (conversion, percent of protonated species: 66, 87; 80, 92), indicating that at these conditions extensive deprotonation takes place and reinitiation (converting "H^+" into the terminal −OH) is rather slow.

Microstructure of Copolymers. The microstructure of copolymers of **B** with **T** was determined by ^{13}C NMR. The proton-decoupled ^{13}C NMR spectrum of the 1:1 statistical copolymer dissolved in benzene-d_6 solvent is shown in Figure 4. Signals corresponding to different heterotriads are clearly visible in regions typical for carbon atoms in the given neighborhood. Signals were assigned on the basis of the relative intensities of different signals of copolymers differing in composition and prepared by different copolymerization procedures. Figure 5 collects these spectra. Thus, in the spectrum of the statistical copolymer with **B**/**T** = 1:3.5 (trace 1 in Figure 5), the following signals are observed: strong signals of the **TTT** triads at 70.6 (OCH_2) and 26.1 ppm (CCH_2C) and much weaker signals of the triad **TBT** at

76.5 (O*C*H) and 29.5 ppm (OCH*C*H$_2$*C*H$_2$CHO) and of the triad **TTB** at 68.0 (**T**−OCH$_2$CH$_2$CH$_2$*C*H$_2$O−**B**), 71.0 (**T**−O*C*H$_2$CH$_2$CH$_2$CH$_2$O−**B**), and 26.5 (**T**−OCH$_2$CH$_2$-CH$_2$*C*H$_2$O−**B**). The signal of the fourth carbon atom of the central unit of the triad **TTB** (**T**−OCH$_2$*C*H$_2$CH$_2$-CH$_2$O−**B**) is hidden under the corresponding signal of the triad **TTT**. Besides, a very weak signal corresponding to the triad **TBB** at 30.2 ppm (**T**−OCH(*C*H$_2$CH$_2$)$_2$-CHO−**B**) is also present. Positions of all signals of heterodiads containing two units of **B** were identified on the basis of the spectrum of the 4:1 **B**/**T** copolymer (trace 2 in Figure 5). Besides signals of the triad **BBB** at 74.5 (O*C*H) and 31.2 ppm (OCH(*C*H$_2$*C*H$_2$)$_2$CHO) and weaker signals corresponding to the triads **TTT**, **TTB**, and **TBT**, described above, strong signals corresponding to the triad **TBB** at 77.1 (**T**−O*C*H(CH$_2$CH$_2$)$_2$CHO−**B**), 30.7 (**T**−OCH(CH$_2$*C*H$_2$)$_2$CHO−**B**), and 30.2 ppm (**T**−OCH(*C*H$_2$CH$_2$)$_2$CHO−**B**) are visible. The fourth signal of the triad **TBB** (**T**−OCH(CH$_2$CH$_2$)$_2$*C*HO−**B**) is overlapped by the signal of the triad **BBB** (at 74.5 ppm). Due to the overlapping of the signals of the triads, it was not possible to determine the contributions of all triads. Thus, microstructure of the copolymers discussed below was based on the following assignments of 10 signals (signals are present in the spectra in the order from left to right):

diads **TB** + **BT** (triads **TBT** + **BBT** + **TBB**)

$$-\mathit{C}\mathrm{HOCH_2}-$$

diad **BB** (triads **TBB** + **BBT** + **BBB**)

$$-\mathit{C}\mathrm{HO}\mathit{C}\mathrm{H}-$$

diad **TT** (triads **TTT** + **TTB** + **BTT**)

$$-\mathit{C}\mathrm{H_2O}\mathit{C}\mathrm{H_2}$$

diads **TB** + **BT** (triads **BTB** + **TTB** + **BTT**)

$$-\mathrm{CHO}\mathit{C}\mathrm{H_2}-$$

triad **BBB**

$$-\mathrm{CHOCH}(\mathit{C}\mathrm{H_2}\mathit{C}\mathrm{H_2})_2\mathrm{CHOCH}-$$

triads **TBB** + **BBT**

$$-\mathrm{CH_2OCH}(\mathit{C}\mathrm{H_2}\mathit{C}\mathrm{H_2})_2\mathrm{CHOCH}-$$

triads **TBB** + **BBT**

$$-\mathrm{CH_2OCH}(\mathrm{CH_2}\mathit{C}\mathrm{H_2})_2\mathrm{CHOCH}-$$

triad **TBT**

$$-\mathrm{CH_2OCH}(\mathit{C}\mathrm{H_2}\mathit{C}\mathrm{H_2})_2\mathrm{CHOCH_2}-$$

diads **TB** + **BT** (triads **BTB** + **BTT** + **TTB**)

$$-\mathrm{CHOCH_2}\mathit{C}\mathrm{H_2}\mathrm{CH_2}\mathrm{CH_2O}-$$

diad **TT** (triads **TTT** + **TTB** + **BTT**)

$$-\mathrm{CH_2OCH_2}\mathit{C}\mathrm{H_2}\mathrm{CH_2}\mathrm{CH_2O}-$$

Statistical Copolymerization of B with T. Statistical copolymerizations of **B** with **T** were carried out at conditions corresponding to living polymerization of **T**. The analysis of the microstructure of the obtained copolymers (cf. microstructure section) performed on the basis of ^{13}C NMR spectra of isolated copolymers indicates that statistical copolymers resemble random ones, with some tendency to alternation.

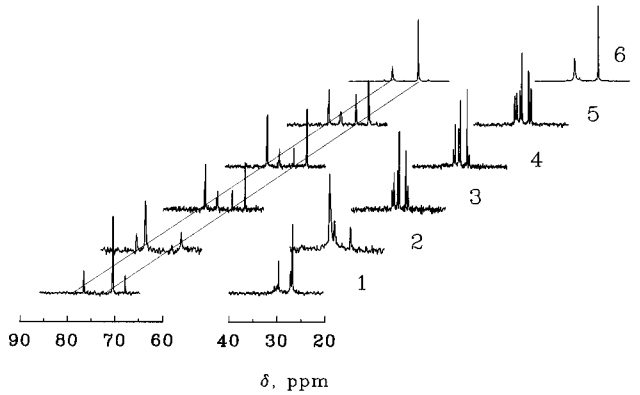

Figure 5. Collection of ^{13}C NMR spectra of copolymers differing by composition and/or copolymerization procedures. Details of copolymerization conditions and microstructure data can be found in Tables 1 and 2 in the rows indicated below (except trace 1: data from ref 6). Trace 1: **T**/**B** = 3.51, statistical copolymerization in CH_2Cl_2 at −23 °C, $[PhCOSbF_6]_0 = 4.5 \times 10^{-2}$, $[\mathbf{T}]_0 = 4.77$, $[\mathbf{B}] = 2.33$ (all in mol L^{-1}); trace 2: **T**/**B** = 0.25, statistical copolymerization, rows 2; trace 3: **T**/**B** = 1, statistical copolymerization, rows 3, trace 4: **T**/**B** = 0.8, statistical copolymerization, rows 4, trace 5: **T**/**B** = 2.2, block copolymerization, method 2, rows 9; trace 6: **T**/**B** = 3, block copolymerization, method 3, rows 12.

Comparison of the ^{1}H NMR spectra (absorption at 5.6 ppm of the protons at the double CC bond of the terminal cyclohexenyl groups) and osmometric measurements show that most of the copolymer chains are terminated with unsaturated units coming from **B** and resulting from the termination reaction.

The number of ester chain ends, originating from initiator residue (when $PhCO^+SbF_6^-$ was used), is lower than calculated. Besides, some $HOCH_2$ end groups were detected (after reaction with trifluoroacetic anhydride) in the ^{1}H NMR spectra.

These results indicate the importance of the termination reaction by proton expulsion as well as suggest that ester end groups, formed in initiation when benzoylium cation is used, are cleaved by protons formed in the termination step (proton expulsion, eq 10). This cleavage possibly proceeds according to the equation shown below (e.g., for the ultimate **T** unit):

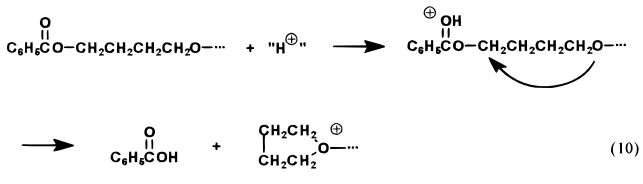

(10)

This reaction is a reinitiation reaction, operating only when ester groups are present in the head−end groups. It does not increase the number of polymer chains and consequently does not decrease the number-average degree of polymerization. Initiation with protonic acids in the absence of ester groups is rather ineffective. The estimated value of the higher limit of the reinitiation rate constant in the mentioned kinetics analysis of copolymerization is also rather low ($k_{rei} < 10^{-5}$ mol^{-1} L s^{-1}).

Table 1. Microstructure of Copolymers Obtained at Different Conditions or by Different Procedures[a]

no.	method[b]	temp (°C)	$[I]_0$ (mol L^{-1})	$[\mathbf{B}]_0$ (mol L^{-1})	$[\mathbf{T}]_0$ (mol L^{-1})	fr(**B**)	fr(**BB**)	fr(**BBB**)	fr(**TBB**) + fr(**BBT**)	fr(**TBT**)	fr(**TT**)
1	s	0	0.045	4.98	0.55	0.86	0.74	0.62	0.22	0.04	0.02
2	s	0	0.047	3.78	0.87	0.81	0.64	0.53	0.21	0.10	0.01
3	s	0	0.039	2.52	2.33	0.53	0.19	0.06	0.26	0.22	0.13
4	s	25	0.071	1.47	1.51	0.56	0.18	0.06	0.25	0.25	0.07
5	b1	25	0.060	3.22	5.29	0.38	0.11	0.03	0.15	0.20	0.34
6	b1	−70/0[c]	0.24	2.55	3.29	0.51	0.29	0.17	0.25	0.1	0.27
7	b1	0	0.036	2.43	3.31	0.45	0.17	0.06	0.21	0.19	0.26
8	b1 + ps	0	0.034	2.7	3.13	0.38	0.15	0.07	0.16	0.15	0.39
9	b2	25	0.066	1.24	3.27	0.31	0.13	0.06	0.13	0.12	0.51
10	b2	25	0.027	0.76	1.27	0.34	0.14	0.06	0.15	0.13	0.46
11	b3	25	0.12	2.00	2.40	0.38	0.30	0.23	0.14	0.03	0.54
12	b3	25	0.065	2.90	1.34	0.25	0.31	0.28	0.065	0.01	0.61
13	p + ps	25	0.01	0.20	0.20	0.16	0.11	0.07	0.07	0.01	0.80
14	p	25	0.01	0.22	0.20	0.53	0.33	0.20	0.26	0.10	0.27

[a] fr(...) denote fractions of different sequences. [b] Methods of preparation: s, statistical copolymerization; b1, b2, and b3, block copolymerizations, methods 1, 2, and 3 (see text); ps, "proton sponge" added; p, homopolymerization of **B** in the presence of poly-**T** ($[-\mathbf{T}-]_0$ instead of $[\mathbf{T}]_0$); solvent, CH_2Cl_2 except no. 12 (CH_3NO_2). [c] After 24 h at −78 °C, the temperature was raised to 0 °C for the next 24 h.

The compositions and microstructures of the obtained copolymers are listed in Table 1 and are discussed in the section describing the distribution of the copolymer units.

Block Copolymerization. In the previous section, we discussed some features of the statistical copolymerization of **B** with **T**. In the present paragraph, we discuss attempts to prepare block copolymers:

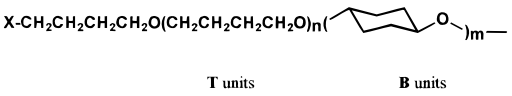

(11)

Experiments were performed in three different ways. According to the first method, polymerization of **T** was brought to equilibrium at a certain temperature (e.g., at room temperature); then the temperature was lowered, in order to decrease the equilibrium **T** concentration, and **B** was added. In this approach, we could expect formation of the block-graded copolymers:

$$(\mathbf{T})_x[(\mathbf{T})_a(\mathbf{B})_b]_y(\mathbf{B})_z$$

...−**T**-homoblock...−...gradient...−...**B**-homoblock−...
copolymer structures

According to the second method, polymerization of **T** was first brought to equilibrium at low temperature (e.g., −20 °C); then the remaining **T** was removed under vacuum at this temperature. Subsequently **B** was introduced and its polymerization, monitored by ^{1}H NMR, was conducted until **B** disappeared. In a typical experiment, first polymerization of **T** ($[\mathbf{T}]_0$ = 7.7 mol L^{-1}) was initiated with $C_6H_5COSbF_6$ (0.087 mol L^{-1}) and conducted at 25 °C for 24 h; then the temperature was lowered to −78 °C, and after an additional 24 h, when according to ^{1}H NMR 10.5% of the initiation amount of **T** was left in the system (after removing monomer), **B** (3.12 mol L^{-1}) was introduced and polymerized for the next 24 h. After this time, a fivefold excess of ammonia in a small volume of CH_3OH was added at the polymerization temperature to kill the active species. Then the copolymer formed was precipitated into CH_3OH. The total ratio of [**T**]/[**B**] in the copolymer was found to be equal to 1.4 (from ^{1}H NMR), whereas the expected ratio (monomer ratio corrected by conversions determined by ^{1}H NMR) was equal to 1.5. The comparison of the calculated and determined $\bar{M}_n$ is as follows: $\bar{M}_n$(calcd) = 10 900; $\bar{M}_n$(VPO) = 13 400; $\bar{M}_n$(GPC) = 9850, ($\bar{M}_w/\bar{M}_n$ = 1.5); $\bar{M}_n$(end groups) = 9400. In a similar experiment, conducted at −20 °C, but with distilling off the remaining **T**, the copolymerization was planned for $\bar{M}_n$ = 5100. The obtained quantities are as follows: content of **B** in copolymer 43%, $\bar{M}_n$(GPC) = 4300 ($\bar{M}_w/\bar{M}_n$ = 1.3), and $\bar{M}_n$(end groups) = 4500 (both copolymers exhibit a large proportion of statistical structures; comparison of the microstructures of these polymers is discussed in the section on the units distribution).

In the third method, poly-**T** terminated on both ends with iodide groups was prepared and then used for block copolymerization. **B** was added after dissolving this polymer in a solvent and then the vial with silver hexafluoroantimonate was broken. In this way, polymerization of **B** was initiated with the active centers located at the ends of the poly-**T** chains. No **T** monomer was present in the system at the beginning of the process. One can say that this method was an improvement over the second method in which the concentration of **T** monomer was decreased substantially in comparison to the first method but some still was present in the system, giving the opportunity to form heterosequences.

The structure of products resulting from the block copolymerization, performed according to the third method, resembles the expected structure of products of a block copolymerization proceeding without side reactions. However, even in these copolymerizations, as discussed in the section on the units distribution, heterosequences characteristic for statistical copolymerization are formed as well. The average length of homo-**T** sequences is much shorter than expected, suggesting again a possibility of cleaving of blocks of **T** units.

At this stage, two explanations were put forward: (i) either the active centers formed from **B** react preferentially with poly-**T** blocks (chain transfer to polymer), cutting them and reshuffling the corresponding units by forming the poly-**T** active species capable of depolymerization as well as **B** addition or (ii) there is an efficient proton transfer from the **B** active species to the poly-**T** blocks, forming the poly-**T** active species upon the attack of **B** (protonated poly-**T** itself is known to be stable).

The third possibility that fast depropagation of **T** blocks can give products resembling so much the statistical copolymers was excluded by the numerical (integration of differential equations) simulation of the

process.) These two mechanisms can be visualized as follows:

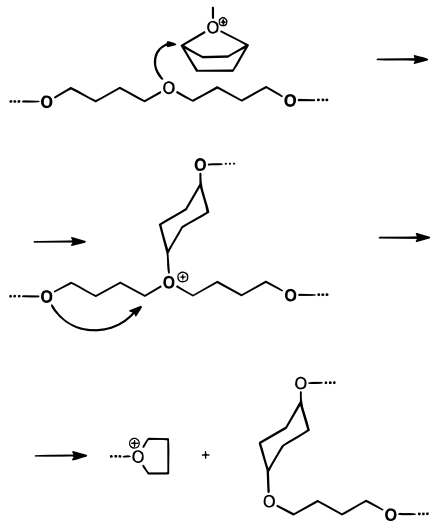

(12)

(anions in this and subsequent schemes are omitted)

These processes (chain transfers to polymer units) would not change the $\bar{M}_n$ but if their rate are comparable to the rate of homopropagation of **B** would exclude a possibility of forming longer blocks. This would thus be a situation similar to the attempted block copolymerization of cyclic acetals, when preparation of the block copolymer is difficult, since the rate of chain transfer is comparable to the chain propagation.[16]

The second mechanism requires first deprotonation of the active species and proton transfer to the poly-**T** block. The deprotonation was indeed observed—one of the copolymer end groups results from deprotonation. Formation of the unsaturated (cyclohexenyl) CC bonds (products of deprotonation of the **B**-type active species) is confirmed by ^{1}H NMR spectra of the products of block copolymerizations (cf. Figure 6). On the basis of comparison of the integral at 5.6 ppm, where the cyclohexenyl end groups absorb:

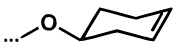

(13)

and the integral of the polymer repeating units, the $\bar{M}_n$ given in the previous paragraph was calculated. Thus, the deprotonation proceeds as the β-elimination process:

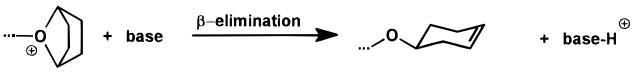

(14)

The strongest bases in the system are comonomers. The fast proton exchange leads eventually to protonated **T** units in homosequences. In one of the proposed mechanisms, the bicyclic secondary oxonium cation hydrogen-bonded to poly-**T** is able to form the tertiary oxonium cation in reaction with the polymer repeating units (preferably intramolecularly), leading finally to the chain scission and formation of the **T**-type active center of propagation (capable of depropagation as well). Another possibility involves the scission of the polymer ether bond directly, due to the attack of monomer on the carbon atom in the α-position to the charged oxygen atom of the secondary oxonium cation, located on the poly-**T** block. These reactions lead to the formation of

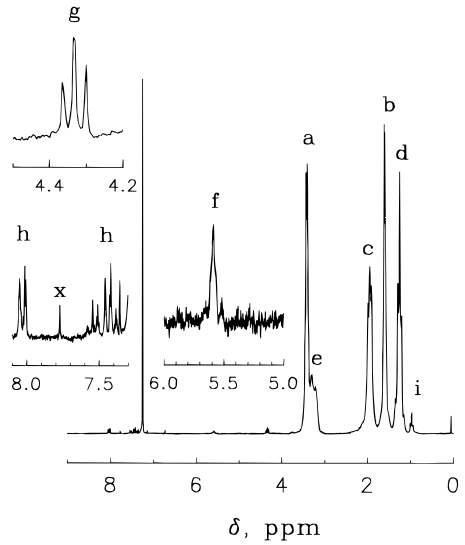

Figure 6. ^{1}H NMR spectrum of the product of block copolymerization (method 1) of **T** and **B**, initiated with $PhCOSbF_6$ and terminated with $(nC_4H_9)_3P$. Copolymerization conditions: 25 °C, CH_2Cl_2 as a solvent, $[I]_0 = 0.24$ mol L^{-1}, $[\mathbf{T}]_0 = 3.29$ mol L^{-1}, $[\mathbf{B}]_0 = 2.55$ mol L^{-1}. Assignments of signals: (a): $-OCH_2CH_2CH_2CH_2O-$; (b) $-OCH_2CH_2CH_2CH_2O-$; (c) axial protons of **B** units: $-OCH(-CH_2CH_2-)_2CH-$; (d) equatorial protons of **B** units: $-OCH(-CH_2CH_2-)_2CH-$; (e) $-CH(-CH_2CH_2-)_2CH-$; (f) olefinic cyclohexene end groups; (g) $C_6H_5C(O)OCH_2CH_2-$; (h) aromatic protons of ester end groups: $C_6H_5C(O)OCH_2-$; (i) end groups originating from the reaction of tributylphosphine with growing active species: $\sim P^+CH_2CH_2CH_2CH_3)_3$.

shorter blocks of **T** in the copolymer and due to subsequent possible depropagation of **B** and **T** to formation of sequences typical for statistical copolymerization, decreasing consequently the blockiness of the formed copolymer:

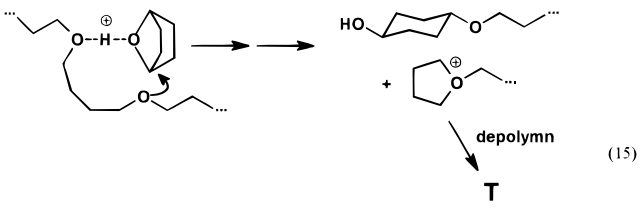

(15)

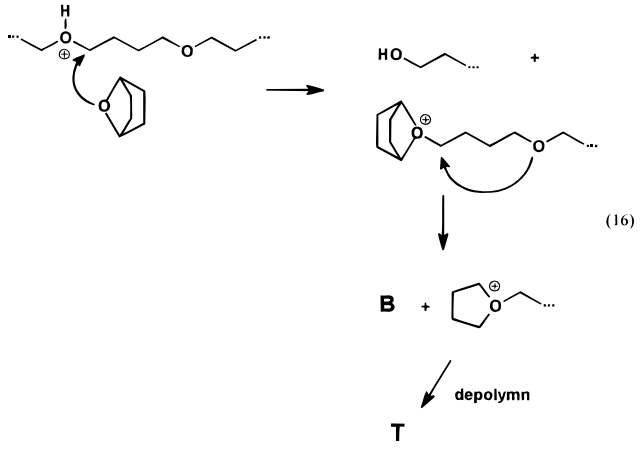

(16)

(17)

As indicated above, the anchimeric assistance can enhance the rates of reactions 15 and 16.

The observation that $\bar{M}_n$(calcd) and $\bar{M}_n$ found from the unsaturated end groups are close to each other seems

Table 2. Fractions of Units B and T Forming Homosequences Fr(X/*n*) and Average Lengths of Homoblocks *L*(X/*n*)[a]

no.	method[b]	Fr(**B**/3)	Fr(**B**/2)	Fr(**T**/2)	*L*(**B**/2)	*L*(**B**/1)	*L*(**T**/1)
1	s	0.72 (0.74)	0.86 (0.86)	0.14 (0.14)	7.2 (8.1)	7.2 (7.1)	1.2 (1.2)
2	s	0.65 (0.66)	0.79 (0.81)	0.05 (0.19)	6.8 (6.3)	4.8 (5.3)	1.06 (1.16)
3	s	0.11 (0.28)	0.35 (0.53)	0.28 (0.47)	2.46 (3.13)	1.56 (2.13)	1.38 (1.89)
4	s	0.11 (0.31)	0.33 (0.56)	0.15 (0.44)	2.47 (3.26)	1.49 (2.26)	1.18 (1.79)
5	b1	0.08 (0.14)	0.29 (0.38)	0.55 (0.62)	2.38 (2.61)	1.41 (1.61)	2.21 (2.63)
6	b1	0.33 (0.26)	0.57 (0.51)	0.55 (0.49)	3.42 (3.04)	2.32 (2.04)	2.23 (1.96)
7	b1	0.13 (0.20)	0.37 (0.45)	0.47 (0.55)	2.57 (2.82)	1.58 (1.62)	1.90 (2.22)
8	b1 + ps	0.18 (0.14)	0.39 (0.38)	0.63 (0.62)	2.83 (2.61)	1.63 (1.61)	2.67 (2.65)
9	b2	0.19 (0.10)	0.42 (0.31)	0.74 (0.69)	2.86 (2.44)	1.72 (1.45)	3.83 (3.22)
10	b2	0.18 (0.12)	0.41 (0.34)	0.70 (0.66)	2.75 (2.52)	1.70 (1.52)	3.30 (2.94)
11	b3	0.60 (0.14)	0.78 (0.38)	0.87 (0.62)	5.35 (2.61)	4.59 (1.61)	7.50 (2.63)
12	b3	0.80 (0.12)	0.89 (0.35)	0.94 (0.65)	10.7 (2.54)	9.2 (1.54)	17.2 (2.86)
13	p + ps	0.46 (0.26)	0.69 (0.16)	0.95 (0.84)	4.06 (2.19)	3.20 (1.19)	21.0 (6.25)
14	p	0.38 (0.28)	0.62 (0.53)	0.57 (0.47)	3.56 (3.13)	2.65 (2.13)	2.35 (1.89)

[a] *n* denotes the length of the shortest homosequences taken into account; data in the table given in parentheses correspond to random copolymers of the same compositions as analyzed copolymers. [b] Cf. Table 1.

to indicate that it is the first mechanism (direct reaction of ~**B*** with poly-**T** blocks) that operates, particularly at lower temperature. If the second mechanism were important, then one could expect reinitiation to be effective and consequently $\bar{M}_n$ lower than $\bar{M}_n$(calcd). Additional confirmation of the hypothesis of the direct attack of active species ~**B*** on sequences of **T** units comes from results of copolymerization and homopolymerization experiments in the presence of the "proton sponge" described in the following section.

Homopolymerization and Block Copolymerization of B in the Presence of the "Proton Sponge". In order to distinguish which of two possible mechanisms is responsible for the cleavage of the homosequences of **T** units in copolymerization, we performed two polymerizations of **B** initiated with $C_6H_5COSbF_6$ in the presence of dead poly-**T**. In one of these experiments, the proton trap 4-methyl-2,6-di-*tert*-butylpyridine ("proton sponge") was added. We assumed that if cleavage of the preformed poly-**T** blocks does not proceed at all during block copolymerization, then only homopolymer of **B** would be formed in both experiments. On the other hand, if only reaction of the active center ~**B*** with the poly-**T** blocks is responsible for reshuffling, and not the proton abstraction, then results of the two experiments should be identical. If however the proton transfer would exclusively be responsible, then reshuffling should only be observed in the absence of the proton trap. Results are presented in rows 7 and 8 of Tables 1 and 2. In both experiments, namely with and without a proton trap, products contain heterosequences, but they differ in the extent of the reshuffling, suggesting that both proton transfer and direct attack of the ~**B*** active species on poly-**T** blocks take place. Indeed, in polymerization of **B** in the presence of poly-**T** (rows 13 and 14 of Tables 1 and 2), in experiments without the proton sponge the average length of homosequences of poly-**T** was shorter than in the experiment with the proton trap: 2.3 without and 21.0 with the proton sponge added, respectively, whereas the initial degree of polymerization of poly-**T** was $\overline{DP}_n$ = 202. This means that during the growth of the poly-**B** block poly-**T** sequences were cut a number of times, approximately 10 times in the presence and approximately 100 times in the absence of a proton trap.

The average lengths of homosequences of **B** units are however similar (3.6 and 4.1, respectively) and much shorter than expected for homopolymerization experiment if attack on poly-**T** were impossible (these would have been equal to 20 and 6.5, respectively). The similar length of the homosequences of **B** units in products obtained in the experiments with and without the proton trap and different lengths of the poly-**T** sequences indicate that the attack of **B**-type active species on homosequences of **T** units takes place together with the proton-transfer reinitiation. In has to be stressed that lower conversion of **B** was observed in the experiment with the proton trap (30−70%) in comparison with 95% without the proton sponge for otherwise the same conditions.

The ratio of the rate constant of homopropagation of **B** (k_{BB}) to the rate constant of the attack of ~**B*** on homosequences of **T** (k_{BpT}) was estimated on the basis of the experiments with homopolymer of **T**. Namely, assuming that in the experiment with the proton sponge the average length is limited almost exclusively by the reaction of ~**B*** with homosequences of **T**, one obtains (cf. Appendix)

$$k_{BB}/k_{BpT} = [L(\mathbf{B}/1) - 1][(\mathbf{TT})]_{av}/[\mathbf{B}]_{av} = 2.4 \quad (18)$$

where L(**B**/1) is the average length of homosequences of **B** units whereas $[(\mathbf{TT})]_{av}$ and $[\mathbf{B}]_{av}$ are the average concentrations of diads **TT** and comonomer **B** in the reacting system. In computations, the arithmetic means of initial and final values were taken.

On the other hand, assuming that the total number of scissions of poly-**T** can be estimated as the ratio of the average lengths of blocks of units **T** at the beginning and at the end of the reaction, one obtains (cf. Appendix)

$$k_{BB}/k_{BpT} = \{[(\mathbf{BB})][(\mathbf{TT})]_{av}L(\mathbf{T}/1)\}/\{[\mathbf{B}]_{av}[(\mathbf{TT})]_0\} = 2.9 \quad (19)$$

where L(**T**/1) is the average length of homosequences of **T** units in product, [(**BB**)] is the concentration of diads **BB** at the end of reaction, and $[(\mathbf{TT})]_0 = \overline{DP}_{n(\text{poly-T})}$ [poly-**T** chains] is the initial concentration of **TT** diads.

These two estimates are close to each other, indicating that the **B**-type active species reacts less than 3 times faster (in CH_2Cl_2 solution) with **B** than with the oxygen atom connecting two units of **T** in homo- or copolymer.

Distribution of the Copolymer Units and the Average Lengths of Homosequences. The extent of blockiness of copolymer can be described by listing determined contributions of fractions of units of the given kind and constituting analyzed homosequences (e.g., diads or triads: Fr(A/2), Fr(A/3); Fr(A/*n*) = fr((A)$_n$)/fr(A) where fr(...) denote molar fractions of units or sequences given in parentheses). In random copolymer these quantities are equal to the corresponding power of the fraction of given units in copolymer, while in block copolymer they are equal to 1, and in alternat-

ing copolymer they are equal to zero since $fr((A)_n) = 0$ ($n > 1$):

	alternating copolymer	random copolymer	block copolymer
$Fr(A/n) =$	$fr((A)_n)/fr(A) = 0$	$[fr(A)]^{n-1}$	1

The closer the discussed quantities are to unity, the higher the tendency to blockiness exhibited in a given copolymer. Blockiness can additionally be characterized by the average lengths of blocks of both kinds, which can be computed from the relationship:

$$L(A/n) = \sum_{i=n}^{\infty} \{i\ fr(B(A)_iB)\} / \sum_{i=n}^{\infty} \{fr(B(A)_iB)\} = n - 1 + fr((A)_n)/fr((A)_nB) \quad (20)$$

where $L(A/n)$ is the number-average length of sequences $(A)_i$, where i is not lower than n (derivation of this equation is given in the Appendix; (a similar equation holds for B units)). For random copolymer, this average length is equal to $L(A/n) = n - 1 + 1/fr(B)$, which gives the average length $L(A/1) = 2$ for 1:1 molar ratio copolymer and separate monomer units considered as the shortest blocks, and $L(A/2) = 3$ when diads are considered as the shortest homosequences.

In the spectrum of the 1:1 **B**/**T** statistical copolymer obtained at high starting comonomer concentrations (Figure 4 and trace 3 in Figure 5), signals corresponding to all triads and expected intensities are visible. On the other hand, when starting comonomer concentrations are low, then the copolymer does not contain any measurable amount of triads **TTT** (trace 4 in Figure 5), which is in agreement with the known high equilibrium monomer concentration of **T** in homopolymerization (~2 mol/L at room temperature). When copolymerization is carried out at a **T** concentration much lower than the equilibrium concentration, then depolymerization of **T**-type active center ~**BTT*** is much faster than homopropagation, while crosspropagation is still sufficiently effective. Consequently, the proportion of **TTT** triads is very low.

The ^{13}C NMR spectrum of the copolymer obtained by addition of **B** monomer to the living homopolymer of **T** after removing most of the **T** monomer from the mixture (second method of block copolymerization; trace 5 in Figure 5) or of the copolymer obtained by the third method of block copolymerization (formation of active species at the ends of poly-**T** chains and instantaneous subsequent polymerization of **B**; trace 6 in Figure 5) exhibit increased intensities of signals of homotriads **TTT** and **BBB**. The fractions of different triads in copolymers obtained at different conditions (or by different procedures) are given in Table 1. In Table 2, the contributions of the monomer units to homosequences and the average lengths of homoblocks are given. The values given in Tables 1 and 2 were calculated on the basis of the analyses of the ^{13}C NMR spectra of corresponding copolymers.

For a better comprehension of the data, the corresponding quantities calculated for the random copolymer of the same compositions are given as well. Thus, when the starting concentration of **T** is much lower than the equilibrium concentration of **T** (for homopolymerization), then the average length of block **T** in the statistical copolymer drops to below 2. Microstructures of the statistical copolymers are, as one could expect, very similar to the microstructure of the random copolymer of the same composition. Nevertheless, some tendency to alternation was observed and in some of the statistical copolymers the average length of homosequences is lower than computed for the random ones. For instance, the average lengths of the homosequences of **B** and **T** units (including monads in calculations) in the statistical copolymer, obtained at 25 °C in CH_2Cl_2 and using the $PhCOCl/AgSbF_6$ initiating system, were found to be 1.49 and 1.18, respectively, whereas for the random copolymer one would have 2.26 and 1.79, respectively.

The most unexpected results are the relatively low fractions of homodiads and relatively short average blocks of both types in copolymers obtained by procedures leading presumably to block copolymers. Due to the reshuffling processes discussed above, copolymers obtained by addition of **B** to living poly-**T**, without removing unreacted monomer (method 1), differ from random copolymers only by slightly higher proportion and slightly longer average lengths of homosequences (cf. rows 5−8 in Tables 1 and 2). When most of the unreacted **T** is removed before adding **B** to living poly-**T** (method 2), then the contribution of homosequences and their average length increase (cf. rows 9 and 10 in Tables 1 and 2).

The highest blockiness was found in copolymers obtained by the third method of block copolymerization, namely, when active species are generated at the chain ends of poly-**T** in reaction mixture containing **B** (rows 12 in Tables 1 and 2). Consequently, the contribution of heterosequences is the lowest. This result can be attributed to the fact that active species of copolymerization are formed in situ at the ends of poly-**T** chains in the system containing no **T** monomer and high concentration of **B**. Application of this method of block copolymerization allowed us to obtain copolymers with enhanced blockiness. For instance, in one of copolymers prepared in CH_2Cl_2 solution, the average lengths of homosequences of **B** and **T** were found to be 4.59 and 7.50, respectively, whereas the corresponding figures for random copolymer of the same composition are 1.61 and 2.63 (rows 11 of the corresponding tables). Even better results were obtained in CH_3NO_2 solution. These presented in rows 12 of the Tables 1 and 2 (e.g., the average lengths of homo-**B** and homo-**T** sequences equal 9.2 and 17.2, respectively, whereas the values expected for random copolymer of the same composition are 1.5 and 2.9). This copolymer is not a diblock, however, but a multiblock copolymer $([(\mathbf{B})_{9.2}(\mathbf{T})_{17.2}]_n$ with $\overline{DP}_n$ not lower than 60.

In the last two rows of Tables 1 and 2 are presented the results of analysis of the microstructures of products of homopolymerization of **B** in the presence of poly-**T** with and without the proton sponge. Formation of heterosequences and computed correspondingly average lengths of homosequences ($L(\mathbf{B}/1) = 3.2$ and 2.7, and $L(\mathbf{T}/1) = 21$ and 2.4, respectively, for products obtained in the presence and in the absence of the proton sponge) allowed estimation of the relative reactivities of ~**B*** in reactions with **B** and with homosequences of **T** units as discussed previously.

Conclusions

Major compositional and kinetic information related to statistical and block copolymerization of 7-oxabicyclo-[2.2.1]heptane (**B**) with THF (**T**) is given. The copolymer composition is mostly governed by the unexpectedly

fast chain transfer of the ~**B*** active species to the poly-**T** segments ($k_{BB}/k_{BpT} \approx 2.5$):

$$\sim\mathbf{B}^* + \mathbf{B} \xrightarrow{k_{BB}} \sim\mathbf{BB}^* \quad (21)$$

$$\sim\mathbf{B}^* + \sim\mathbf{TT}\sim \xrightarrow{k_{BpT}} \sim\mathbf{T}^* + \sim\mathbf{BT}\sim \quad (22)$$

This phenomenon, well known in the polymerization of cyclic acetals, is so important because ~**B*** is much more reactive than ~**T*** ($k_{BT}/k_{TT} \approx 10$ and $k_{BB}/k_{TB} \approx 7$). The higher reactivity of ~**B*** is due to its higher ring strain than the strain of ~**T***.

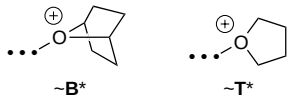

Thus, pure block copolymers could not be obtained. Nevertheless, multiblocks with promesogenic units $(\mathbf{B})_m$ have been prepared, with a composition like $[(\mathbf{T})_n(\mathbf{B})_m]_q$, where $n \approx 9$, $m \approx 17$, and $q \approx 3$.

Acknowledgment. This work was financed by a grant from the State Committee of Scientific Research (KBN), No. 7 7728-9203.

Appendix

Differential Equations Used in Kinetic Analysis of Copolymerization. The set of differential equations describing the discussed copolymerization was formulated as follows. First, the equations for changes of concentrations of comonomers and active species are expressed as functions of concentrations of the corresponding reagents (rate constants are defined by the reaction scheme (1)−(9)):

$$d[\mathbf{T}]/dt = -(k_{TT}[\mathbf{T}][\sim\mathbf{T}^*] + k_{BT}[\mathbf{T}][\sim\mathbf{B}^*] - k_{-TT}[\sim\mathbf{TT}^*] - k_{-BT}[\sim\mathbf{BT}^*]) \quad (A1)$$

$$d[\mathbf{B}]/dt = -(k_{BB}[\mathbf{B}][\sim\mathbf{B}^*] + k_{TB}[\mathbf{B}][\sim\mathbf{T}^*] - k_{-BB}[\sim\mathbf{BB}^*] - k_{-TB}[\sim\mathbf{TB}^*]) \quad (A2)$$

$$d[\sim\mathbf{T}^*]/dt = k_{BT}[\sim\mathbf{B}^*][\mathbf{T}] + k_{-TB}[\sim\mathbf{TB}^*] - k_{TB}[\sim\mathbf{T}^*][\mathbf{B}] - k_{-BT}[\sim\mathbf{BT}^*] \quad (A3)$$

$$d[\sim\mathbf{B}^*]/dt = -k_{BT}[\sim\mathbf{B}^*][\mathbf{T}] - k_{-TB}[\sim\mathbf{TB}^*] + k_{TB}[\sim\mathbf{T}^*][\mathbf{B}] + k_{-BT}[\sim\mathbf{BT}^*] - k_{ter}[\sim\mathbf{B}^*] + k_{rei}([\sim\mathbf{X}^*]_0 - [\sim\mathbf{X}^*]) \quad (A4)$$

$$d[\sim\mathbf{X}^*]/dt = -k_{ter}[\sim\mathbf{B}^*] + k_{rei}([\sim\mathbf{X}^*]_0 - [\sim\mathbf{X}^*])[\mathbf{B}] \quad (A5)$$

where $[\sim\mathbf{X}^*] = [\sim\mathbf{B}^*] + [\sim\mathbf{T}^*]$ and $([\sim\mathbf{X}^*]_0 - [\mathbf{X}^*])$ is the concentration of free protons.

$$d[\sim\mathbf{TT}^*]/dt = k_{TT}[\sim\mathbf{BT}^*][\mathbf{T}] - k_{-TT}[\sim\mathbf{BTT}^*] + k_{-TB}[\sim\mathbf{TTB}^*] - k_{TB}[\sim\mathbf{TT}^*][\mathbf{B}] \quad (A6)$$

$$d[\sim\mathbf{BB}^*]/dt = k_{BB}[\sim\mathbf{TB}^*][\mathbf{B}] - k_{-BB}[\sim\mathbf{TBB}^*] + k_{-BT}[\sim\mathbf{BBT}^*] - k_{BT}[\sim\mathbf{BB}^*][\mathbf{T}] - k_{ter}[\sim\mathbf{BB}^*] \quad (A7)$$

Then it was assumed that the conditional probabilities of preceding given units by units of the same kind are independent of the position of the unit in the polymer chain (at least at the chain end):

$$p_{TT} = [\sim\mathbf{TT}^*]/[\sim\mathbf{T}^*] = [\sim\mathbf{TTY}^*]/[\sim\mathbf{TY}^*] \quad (A8)$$

$$p_{BB} = [\sim\mathbf{BB}^*]/[\sim\mathbf{B}^*] = [\sim\mathbf{BBY}^*]/[\sim\mathbf{BY}^*] \quad (A9)$$

where $\mathbf{Y} = \mathbf{T}$ and/or $\mathbf{B}$.

Consequently, the following relationships hold:

$$dp_{TT}/dt = \{(d[\sim\mathbf{TT}^*]/dt) + p_{TT}(d[\sim\mathbf{T}^*]/dt)\}/[\sim\mathbf{T}^*] \quad (A10)$$

$$dp_{BB}/dt = \{(d[\sim\mathbf{BB}^*]/dt) + p_{BB}(d[\sim\mathbf{B}^*]/dt)\}/[\sim\mathbf{B}^*] \quad (A11)$$

Introduction as new variables fractions of active species of different types ($x_T = [\sim\mathbf{T}^*]/[\sim\mathbf{X}^*]$,

$$x_B = [\sim\mathbf{B}^*]/[\sim\mathbf{X}^*])$$

one can now formulate the final set of differential equations by combining the above presented equations:

$$d[\sim\mathbf{X}^*]/dt = -k_{ter}[\sim\mathbf{X}^*]x_B + k_{rei}([\sim\mathbf{X}^*]_0 - [\sim\mathbf{X}^*])[\mathbf{B}] \quad (A12)$$

$$dx_T/dt = (1 - x_T)\{k_{BT}[\mathbf{T}] + k_{-TB}(1 - p_{BB})\} - x_T\{k_{TB}[\mathbf{B}] + k_{-BT}(1 - p_{TT})\} - x_T\{-k_{ter}x_B + k_{rei}([\sim\mathbf{X}^*]_0/[\sim\mathbf{X}^*] - 1)\} \quad (A13)$$

$$d[\mathbf{T}]/dt = -[\sim\mathbf{X}^*]\{x_T(k_{TT}[\mathbf{T}] - k_{-TT}p_{TT} - k_{-BT}(1 - p_{TT})) + (1 - x_T)k_{BT}[\mathbf{T}]\} \quad (A14)$$

$$d[\mathbf{B}]/dt = -[\sim\mathbf{X}^*]\{(1 - x_T)(k_{BB}[\mathbf{B}] - k_{-BB}p_{BB} - k_{-TB}(1 - p_{BB})) + x_Tk_{TB}[\mathbf{B}])\} \quad (A15)$$

$$dp_{TT}/dt = \{k_{TT}(1-p_{TT})x_T[\mathbf{T}] - k_{-TT}p_{TT}(1 - p_{TT})x_T + 2\,k_{-TB}(1 - p_{BB})p_{TT}(1 - x_T) - 2\,k_{TB}p_{TT}x_T[\mathbf{B}] + k_{BT}p_{TT}(1-x_T)[\mathbf{T}] - k_{-BT}p_{TT}(1 - p_{TT})x_T\}/x_T \quad (A16)$$

$$dp_{BB}/dt = \{k_{BB}(1 - p_{BB})(1 - x_T)[\mathbf{B}] - k_{-BB}p_{BB}(1 - p_{BB})(1 - x_T) + 2\,k_{-BT}p_{BB}(1 - p_{TT})x_T - 2\,k_{BT}p_{BB}(1 - x_T)[\mathbf{T}] - k_{ter}p_{BB}(1 - x_T) - k_{-TB}p_{BB}(1 - p_{BB})(1 - x_T) + k_{TB}p_{BB}x_T[\mathbf{B}] - k_{ter}p_{BB}(1 - x_T) + k_{rei}p_{BB}[\mathbf{B}]([\sim\mathbf{X}^*]_0/[\sim\mathbf{X}^*] - 1)\}/(1 - x_T) \quad (A17)$$

Numerical Integration and Fitting of the Experimental Data. The equation set (A12)−(A17) could be solved by numerical integration. The estimation of the rate constants was performed by the least squares fitting of results of integration for the assumed values of rate constants to the experimental data. Both integration and fitting were done using the program Scientist (integration according to the Adams method). At the beginning, the least squares fitting initial values of the rate constants for both commonomers were assumed equal to those known for homopolymerization of **T**[17] and expected for **B**; k_{ter} and k_{rei} were first used as equal to 10^{-6} (s^{-1} and mol^{-1} L s^{-1}, respectively). In the first step of fitting, all rate constants but k_{BB} and k_{-BB} were kept constant. In the second step of fitting, rate constants of heteropropagations were allowed to vary. In the next steps of fitting, various rate constants

were varied (two or three rate constants simultaneously in different sets) until no better fit could be obtained. The procedure of fitting was repeated several times, changing rate constants in different orders. The reported values of the rate constants are those giving the best fit and the estimated possible errors are equal to the standard deviations of the results obtained in six different fittings.

Derivations of Eqs 18−20. The average length of blocks of **B** units (in a polymerization system of B in the presence of poly-**T**) is equal to the ratio of the overall consumption of **B** and of consumption of diads **TT** (scission of poly-**T**):

$$L(\mathbf{B}/1) = \frac{\int_0^t (k_{BB}[\sim\mathbf{B}^*][\mathbf{B}] + k_{TB}[\sim\mathbf{T}^*][\mathbf{B}])\,\mathrm{d}t}{\int_0^t k_{BpT}[\sim\mathbf{B}^*][\mathbf{TT}]\,\mathrm{d}t} \quad \text{(A18)}$$

Assuming steady-state conditions for interconversions of active species

$$\frac{\mathrm{d}[\sim\mathbf{B}^*]}{\mathrm{d}t} = -k_{BpT}[\sim\mathbf{B}^*][\mathbf{TT}] + k_{TB}[\sim\mathbf{T}^*][\mathbf{B}] = 0 \quad \text{(A19)}$$

and approximating the integrals by the products of the average rates of the corresponding reactions and the time intervals, one gets

$$L(\mathbf{B}/1) = \frac{(k_{BB}[\sim\mathbf{B}^*]_{av}[\mathbf{B}]_{av} + k_{BpT}[\sim\mathbf{B}^*]_{av}[\mathbf{TT}]_{av})\Delta t}{k_{BpT}[\sim\mathbf{B}^*]_{av}[\mathbf{TT}]_{av}\Delta t} \quad \text{(A20)}$$

Consequently,

$$L(\mathbf{B}/1) = \frac{k_{BB}[\mathbf{B}]_{av}}{k_{BpT}[\mathbf{TT}]_{av}} + 1 \quad \text{(A21)}$$

$$\frac{k_{BB}}{k_{BpT}} = (\mathrm{L}(\mathbf{B}/1) - 1)[\mathbf{TT}]_{av}/[\mathbf{B}]_{av} \quad \text{(eq 18)} \quad \text{(A22)}$$

On the other hand, the decrease of concentration of diads **TT** is proportional to the ratio of the initial and final lengths of blocks of units **T** as well as to the concentration of polymer chains:

$$-\Delta[\mathbf{TT}] = \int_0^t k_{BpT}[\sim\mathbf{B}^*][\mathbf{TT}]\,\mathrm{d}t = \frac{\overline{\mathrm{DP}}_{n,\text{poly-T}}}{L(\mathbf{T}/1)}[\text{poly-}\mathbf{T}\text{ chains}]_0 = \frac{[\mathbf{TT}]_0}{L(\mathbf{T}/1)} \quad \text{(A23)}$$

and the concentration of diads **BB** depends on the rate of homopropagation:

$$[\mathbf{BB}] = \int_0^t k_{BB}[\sim\mathbf{B}^*][\mathbf{B}]\,\mathrm{d}t \quad \text{(A24)}$$

Approximating integrals with the corresponding functions of average concentrations, one gets

$$k_{BpT}[\sim\mathbf{B}^*]_{av}[\mathbf{TT}]_{av}\Delta t = \frac{[\mathbf{TT}]_0}{L(\mathbf{T}/1)} \quad \text{(A25)}$$

$$k_{BB}[\sim\mathbf{B}^*]_{av}[\mathbf{B}]_{av}\Delta t = [\mathbf{BB}] \quad \text{(A26)}$$

$$\frac{k_{BB}}{k_{BpT}} = \frac{[\mathbf{BB}]\,L(\mathbf{T}/1)\,[\mathbf{TT}]_{av}}{[\mathbf{TT}]_0[\mathbf{B}]_{av}} \quad \text{(eq 19)} \quad \text{(A27)}$$

The average length of a block of units of the same type, considering blocks not shorter than n, can be computed from the equation derived below (assuming $\overline{\mathrm{DP}}_n \to \infty$):

$$L(\mathrm{A}/n) = \frac{\sum_{i=n}^{\infty} i\ \mathrm{fr}(\mathrm{BA}_i\mathrm{B})}{\sum_{i=n}^{\infty} \mathrm{fr}(\mathrm{BA}_i\mathrm{B})} = \frac{\sum_{i=n}^{\infty} \{i\ \mathrm{fr}(\mathrm{BA}_i) - i\ \mathrm{fr}(\mathrm{BA}_{i+1})\}}{\sum_{i=n}^{\infty} \{\mathrm{fr}(\mathrm{BA}_i) - \mathrm{fr}(\mathrm{BA}_{i+1})\}} = \frac{(n-1)\ \mathrm{fr}(\mathrm{BA}_n) + \sum_{i=n}^{\infty} i\ \mathrm{fr}(\mathrm{BA}_i\mathrm{B})}{\mathrm{fr}(\mathrm{BA}_n)} = n - 1 + \frac{\sum_{i=n}^{\infty} \{\mathrm{fr}(\mathrm{A}_i) - \mathrm{fr}(\mathrm{A}_{i+1})\}}{\mathrm{fr}(\mathrm{BA}_n)} \quad \text{(A28)}$$

$$L(\mathrm{A}/n) = n - 1 + \frac{\mathrm{fr}(\mathrm{A}_n)}{\mathrm{fr}(\mathrm{BA}_n)} \quad \text{(eq 20)} \quad \text{(A29)}$$

For random copolymer $\mathrm{fr}(\mathrm{A}_n) = [\mathrm{fr}(\mathrm{A})]^n$, $\mathrm{fr}(\mathrm{BA}_n) = \mathrm{fr}(\mathrm{B})[\mathrm{fr}(\mathrm{A})]^n$,

$$L(\mathrm{A}/n) = n - 1 + 1/\mathrm{fr}(\mathrm{B}) \quad \text{(A30)}$$

References and Notes

(1) Wittbecker, E. L.; Hall, H. K., Jr.; Campbell, T. W. *J. Am. Chem. Soc.* **1960**, *82*, 1218.
(2) Kops, J.; Spanggaard, H. *Makromol. Chem.* **1972**, *151*, 21.
(3) Kops, J.; Spanggaard, H. *Polym. Bull.* **1986**, *16*, 507.
(4) Percec, V. *Makromol. Chem., Macromol. Symp.* **1988**, *13/14*, 397.
(5) Paci, M.; Andruzzi, F.; Ceccarelli, G. *Macromolecules* **1982**, *15*, 835.
(6) Sikkema, D. J.; Hoogland, P. *Polymer* **1986**, *27*, 1443.
(7) Libiszowski, J.; Szymanski, R.; Penczek, S. *Macromol. Rapid Commun.* **1995**, *16*, 687.
(8) Olah, G. A.; Kuhn, S. J.; Tolgyesi, W. S.; Baker, E. B. *J. Am. Chem. Soc.* **1962**, *84*, 2733.
(9) Duda, A.; Florjanczyk, Z.; Hofman, A.; Slomkowski, S.; Penczek, S. *Macromolecules* **1990**, *23*, 1640.
(10) Brzezinska, K.; Chwialkowska, W.; Kubisa, P.; Matyjaszewski, K.; Penczek, S. *Makromol. Chem.* **1977**, *178*, 2491.
(11) Penczek, S.; Kubisa, P.; Matyjaszewski, K. *Adv. Polym. Sci.* **1980**, *37*, 1.
(12) Rosenberg, B. A.; et al. *J. Polym. Sci.* **1964**, *C16*, 1917.
(13) Dreyfuss, P.; Dreyfuss, M. P. *Adv. Polym. Sci.* **1967**, *4*, 428.
(14) Bawn, C. E.; Bell, R. M.; Ledwith, A. *Polymer* **1965**, *6*, 95.
(15) Matyjaszewski, K.; Slomkowski, S.; Penczek, S. *J. Polym. Sci., Polym. Chem. Ed.* **1979**, *17*, 2413.
(16) Chwialkowska, W.; Kubisa, P.; Penczek, S. *Makromol. Chem.* **1982**, *183*, 753.
(17) Penczek, S.; Kubisa, P.; Matyjaszewski, K. *Adv. Polym. Sci.* **1985**, *68/69*, 1.

MA951183Q